Supporting Information

Modular Assembly of MOF-derived Carbon Nanofibers into Macroarchitectures for Water Treatment.

Zishi Zhang, Chaohai Wang*, Yiyuan Yao, Hao Zhang, Jongbeom Na, Yujun Zhou, Zhigao Zhu, Junwen Qi, Miharu Eguchi, Yusuke Yamauchi*, Jiansheng Li*

Z. Zhang, Dr. C. Wang, Y. Yao, H. Zhang, Dr. Y. Zhou, Prof. Z. Zhu, Prof. J. Qi, and Prof. J. Li
Jiangsu Key Laboratory of Chemical Pollution Control and Resources Reuse, School of Environmental and Biological Engineering, Nanjing University of Science and Technology, Nanjing 210094, People's Republic of China.
E-mail: wch2016@njust.edu.cn, lijsh@njust.edu.cn

Dr. J. Na, Dr. Miharu Eguchi, Prof. Y. Yamauchi
Australian Institute for Bioengineering and Nanotechnology (AIBN) and School of Chemical Engineering, The University of Queensland, Brisbane, QLD 4072, Australia
E-mails: y.yamauchi@uq.edu.au

Dr. J. Na
Materials Architecturing Research Center, Korea Institute of Science and Technology, Seoul 02792, Republic of Korea

Dr. Miharu Eguchi, Prof. Y. Yamauchi
JST-ERATO Yamauchi Materials Space-Tectonics Project and International Center for Materials Nanoarchitectonics (WPI-MANA), National Institute for Materials Science (NIMS), 1-1 Namiki, Tsukuba, Ibaraki 305-0044, Japan

Experimental methods

Materials. $Zn(NO_3)_2{\cdot}6H_2O$, 2-methylimidazole (2-MeIM), cetyltrimethylammoniumbromide (CTAB), polyacrylonitrile (PAN, MW = 150,000), polyvinylpyrrolidone-K30 (PVP-K30) were purchased from Sigma-Aldrich. N,N-dimethylformamide (DMF, ≥99.9%), *tert*-butyl alcohol (TBA), toluene, ethyl acetate, ethylene glycol, tetrahydrofuran (THF), chloroform, carbon tetrachloride, pump oil, n-hexane, cyclohexane, methanol, and ethanol were purchased from Nanjing Chemical Reagent Co., Ltd. Vegetable (veg) oil was purchased from Suguo Supermarkets. All chemicals were used without further purification.

Preparation of ZIF-8 nanoparticles. 21.6 g 2-MeIM was dissolved in 342 mL of Deionized (DI) water; 8.0 mL of 0.01 M CTAB was added to the 2-MeIM solution with stirring for 10 min. Then, 1.4g $Zn(NO_3)_2{\cdot}6H_2O$ in 50 ml of DI water was rapidly added to the above solution with stirring for another 3 h at room temperature. The white product was collected by centrifugation (10000 rpm, 8 min) and washed with DI water for three times; Finally, the powder was dried under vacuum for 12 h at 80°C.

Synthesis of ZIF-8/PAN/PVP nanofibers (NFs). Typically, 0.6 g ZIF-8 powder was dissolved in 5.5 mL DMF with sonication until it was well dispersed. Then, 0.4 g PAN and 0.4 PVP were added into the solution with stirring at 65°C for 3 h to obtain the electrospinning precursor. The electrospinning process was carried out by applying a high positive voltage (10.0 kV) at a collecting distance of 15 cm. The injection speed was fixed at 0.08 mm min^{-1}.

Fabrication of ZIF-8/nanofiber aerogels (NFAs), preoxidized ZIF-8/NFAs, C-ZIF-8-carbon nanofiber aerogels (CNFAs). The ZIF-8/PAN/PVP nanofiber membrane (1.14 g) was cut into small pieces (1 cm × 1 cm) and were dispersed in 100 mL water/*tert*-butanol mixture solvents (volume ratio of 3:1). The mixture was homogenzied for 10 min at 30000 rpm using a homogenizer. The uniform nanofiber dispersion was transferred into molds and frozen in the fridge for 12 h. Subsequently, the frozen samples were freeze-dried for 48 h to obtain ZIF-8/NFAs. NFAs were also fabricated under the same conditions without the addition of ZIF-8 nanoparticles. ZIF-8/NFAs (NFAs) were pre-oxidized at 250°C for 1 h and annealed at 900°C for 3 h under N_2 atmosphere to obtain C-ZIF-8-CNFAs (CNFAs). The temperature can affect the surface area and microstructure of ZIF-8 derived carbon. Based on our previous study on ZIF-8 derived carbon, it is found that 900°C is the most suitable for ZIF-8 derived carbon aerogels, since the carbonization process is terminated, and the Zn content can be evaporated completely.

Characterization. The structure and morphology of the samples were investigated by transmission electron microscopy (TEM, FEI Tecnai 20) and scanning electron microscope (SEM, FEI 250 and JEOL 7800). The X-ray photoelectron spectroscopy (XPS) spectra were obtained by using a PHI Quantera Ⅱ ESCA System

with Al Kα radiation at 1486.8V. N_2 adsorption and desorption isotherms were measured using a Micromeritics ASAP-2020 instrument. The specific surface area and the pore size distribution were calculated by using the Brunauer-Emmett-Teller (BET) and Density Functional Theory (DFT) method, respectively. The crystal configuration and composition were examined by XRD (BRUKER D8, Cu Kα) at 40 kV and 40 mA. Raman spectra were collected on Renishaw in Via reflex spectrometer system. The compression experiments were tested using an UTM 2203 universal machine with 100-N load cells at a strain rate of 3 mm min^{-1} for σ-ε tests and of 3 mm min^{-1} for 50 cyclic fatigue tests. Water contact angles of samples were measured using a contact angle system (OCA20, Dataphysics Instruments, Germany) at room temperature using a water droplet (10 μL) as an indicator. The hydrophilicity of the samples was characterized by a contact Angle measurement system (WCA, KrussdSA30, Germany).

Absorption measurement. The samples were soaked in the different organic solvents and oils, stayed for 5 min at the room temperature. The absorption capacity of samples (Q) for or organic solvents (oils) was calculated from the weights (wt) of samples before and after absorption, using the following Eq.

$$Q = \left(wt_{after} - wt_{before}\right) / wt_{before}$$

where wt_{after} is the weight of CAs at absorption equilibrium (mg) and wt_{before} is the weight of CAs before absorption (mg).The recyclability test was performed in ethanol. The adsorbed organic solvents were easily extracted by heating treatment (at 100°C for 2 hours) due to weak interaction between the solvents and porous carbon aerogel. The weight was measured in the same method.

Solar vapor generation measurement. The sample was vertically immobilized within a block of floating polystyrene foam, and the bottom part (thickness: 5 mm) was immersed within bulk water to ensure stable water supply during the evaporation process. The evaporation mass change was measured by an electronic balance under solar irradiation of 1 kW m^{-2} (1 sun).

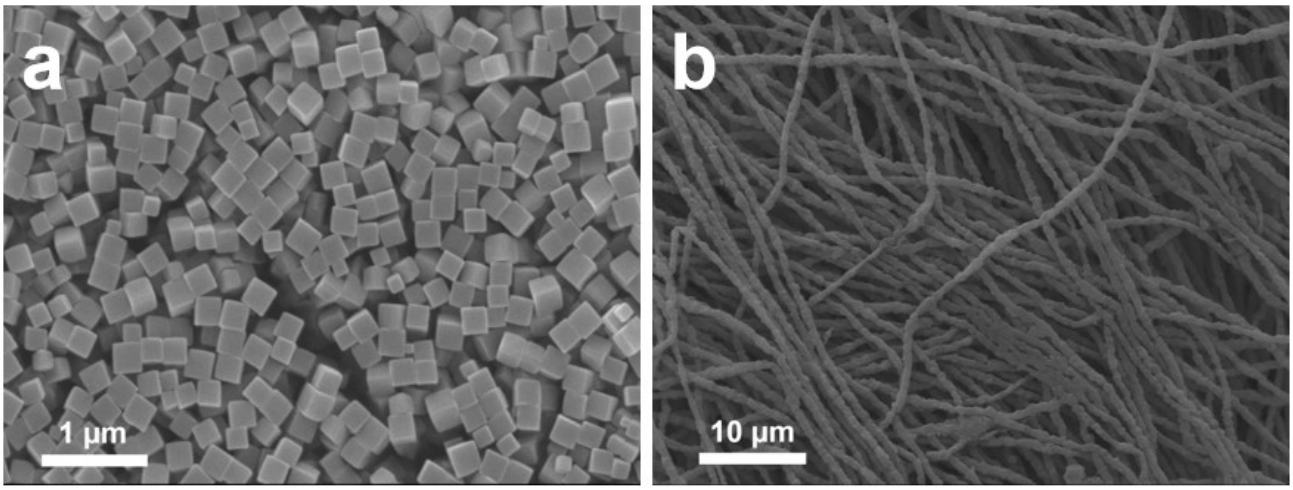

Figure S1 (a,b) SEM images of ZIF-8 nanoparticles and ZIF-8/nanofibers.

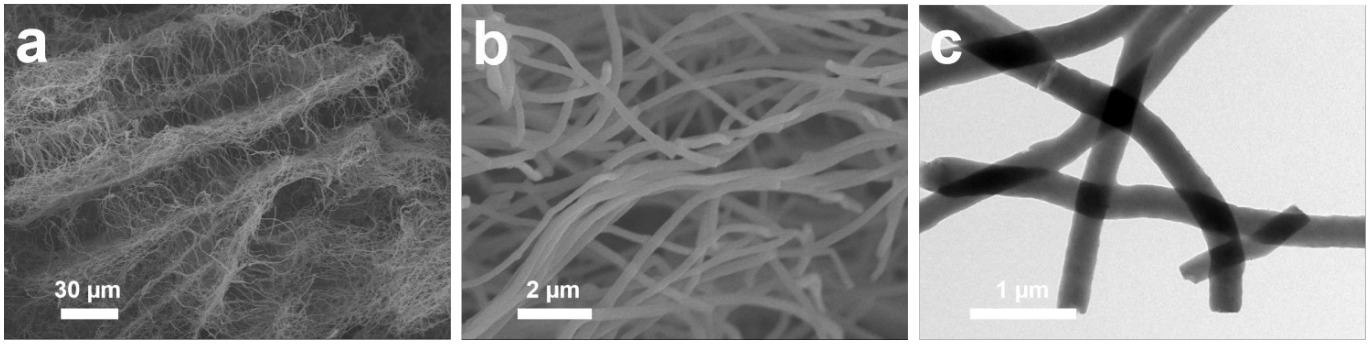

Figure S2 (a–c) SEM (a,b) and TEM (c) images of CNFAs.

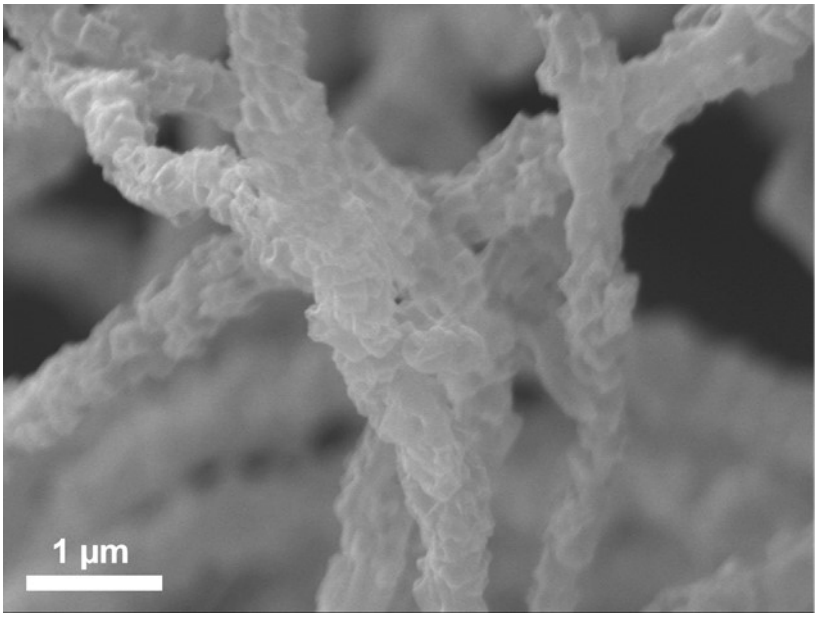

Figure S3 SEM image of C-ZIF-8-CNFAs.

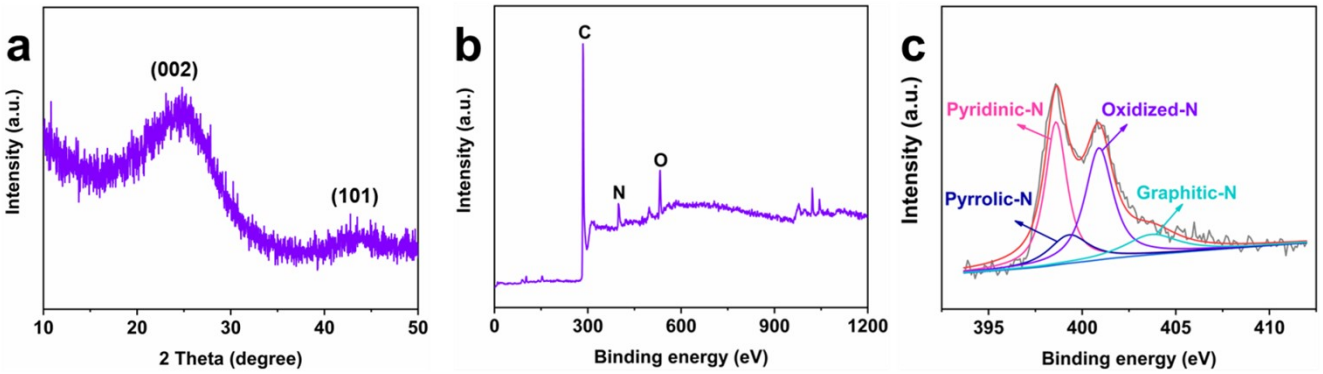

Figure S4 (a) Wide-angle XRD pattern of C-ZIF-8-CNFAs. (b) XPS spectrum. (c) High-resolution N 1s spectra.

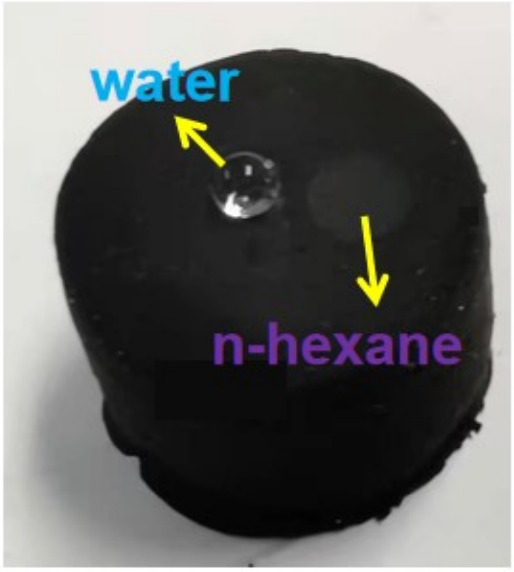

Figure S5 Photograph of the droplets of water and n-hexane on the C-ZIF-8-CNFAs surface.

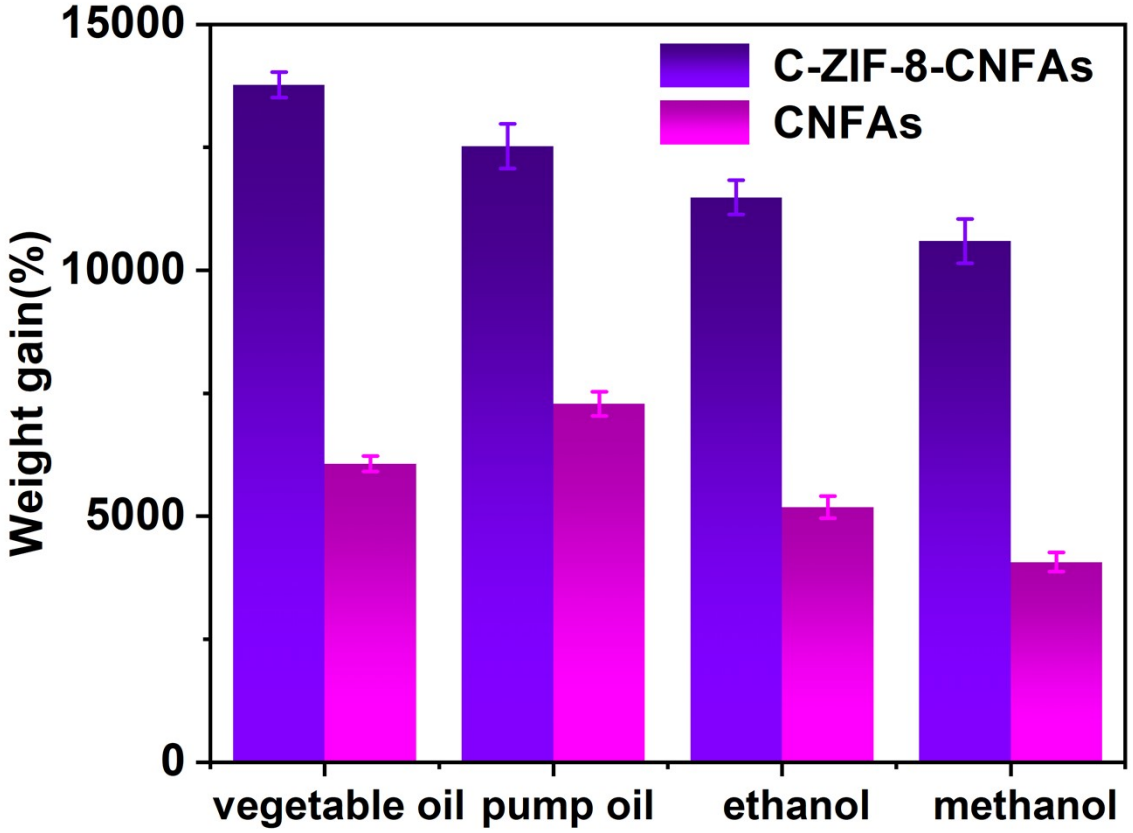

Figure S6 Absorption efficiency of C-ZIF-8-CNFAs and CNFAs for typical organic solvents and oils.

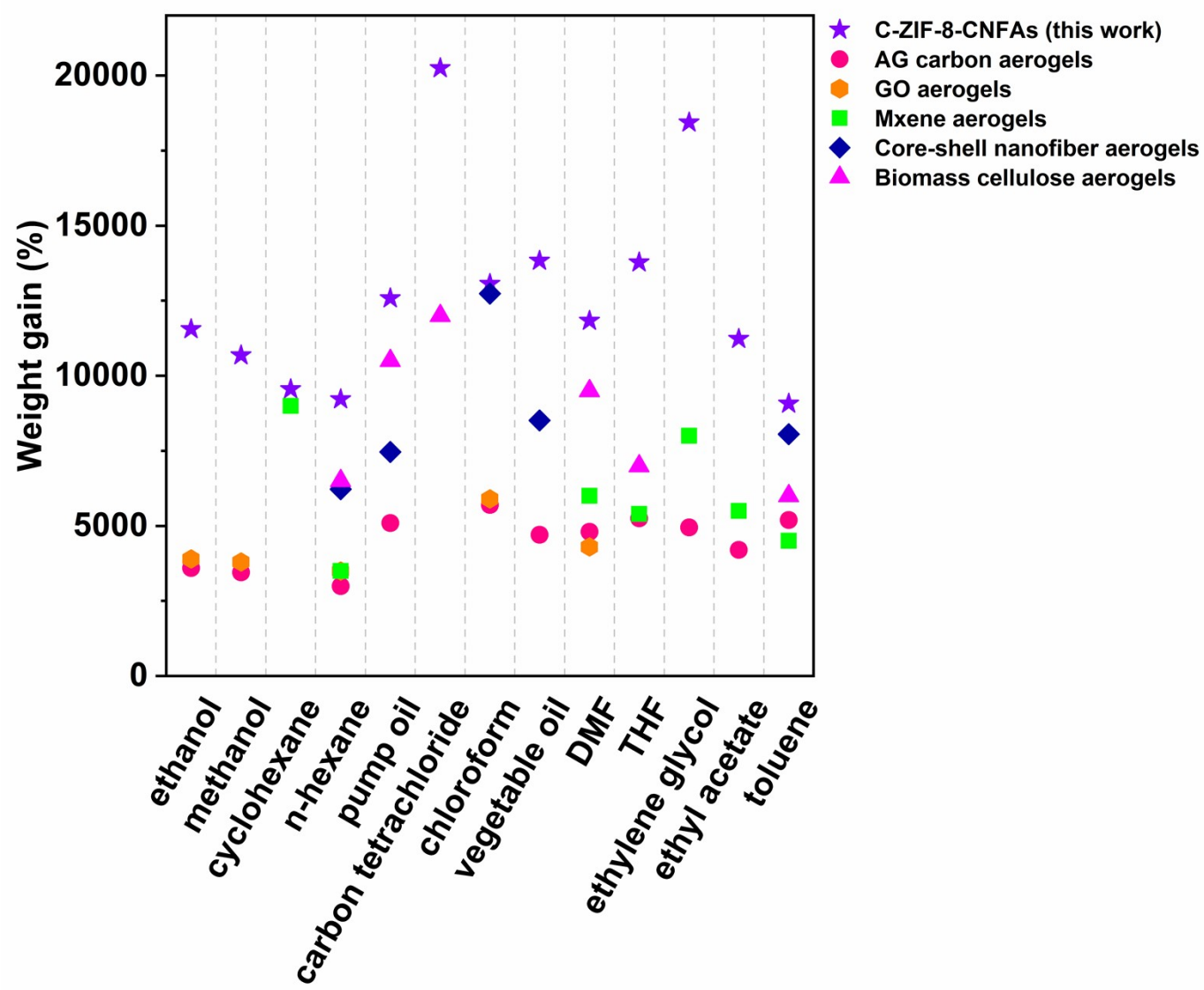

Figure S7 Comparison of the adsorption capacities of previously reported aerogels towards typical adsorbents. (AG carbon aerogels[1]; GO aerogels[2]; Mxene aerogels[3]; Core-shell nanofiber aerogels[4]; Biomass cellulose aerogels[5].)

References

[1] C. H. Wang, J. Kim, J. Tang, J. Na, Y. M. Kang, M. Kim, H. Lim, Y. Bando, J. S. Li, Y. Yamauchi, *Angew. Chem. Int. Ed.* **2020**, *59*, 2066-2070.

[2] J. J. Mao, M. Z. Ge, J. Y. Huang, Y. K. Lai, C. J. Lin, K. Q. Zhang, K. Meng, Y. X. Tang, *J. Mater. Chem. A* **2017**, *5*, 11873-11881.

[3] T. X. Shang, Z. F. Lin, C. S. Qi, X. C. Liu, P. Li, Y. Tao, Z. T. Wu, D. W. Li, P. Simon, Q. H. Yang, *Adv. Funct. Mater.* **2019**, *29,* 1903960.

[4] G. J. Jiang, J. Y. Ge, Y. X. Jia, X. Y. Ye, L. Y. Jin, J. R. Zhang, Z. P. Zhao, G. F. Yang, L. X. Xue, S. Xie, *Sep. Purif. Technol.* **2021**, *270,* 118740.

[5] D. S. Yuan, T. Zhang, Q. Guo, F. X. Qiu, D. Y. Yang, Z. P. Ou, *Chem. Eng. J.* **2018**, *351*, 622-630.

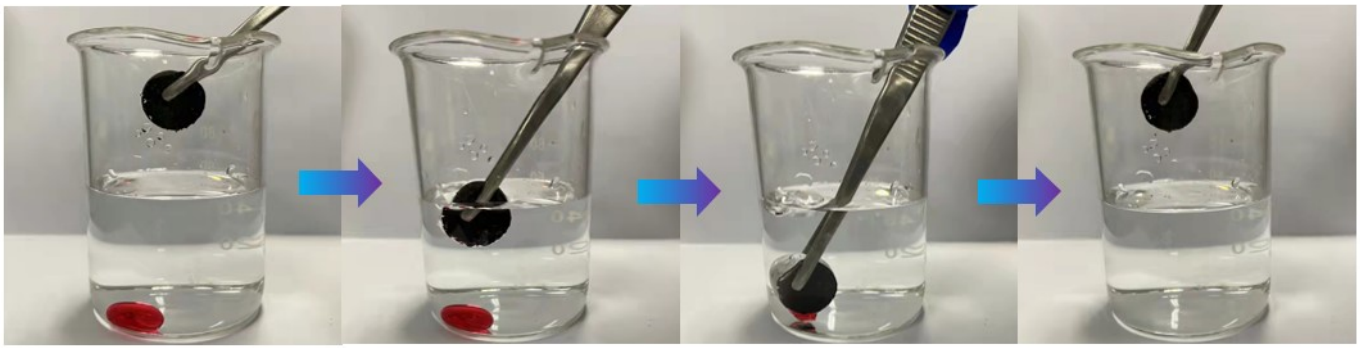

Figure S8 Removal of carbon tetrachloride at the bottom of water.

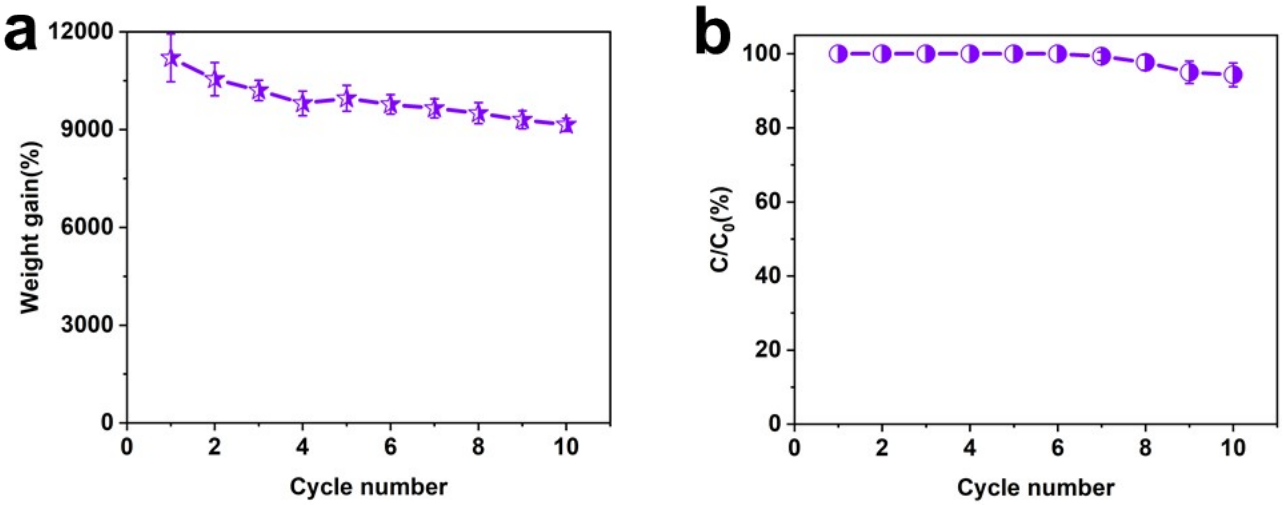

Figure S9 (a) Recyclability tests for the absorption capacity of C-ZIF-8-CNFAs for ethanol. (b) The mass change of C-ZIF-8-CNFAs during the cyclic adsorption experiment for ethanol.

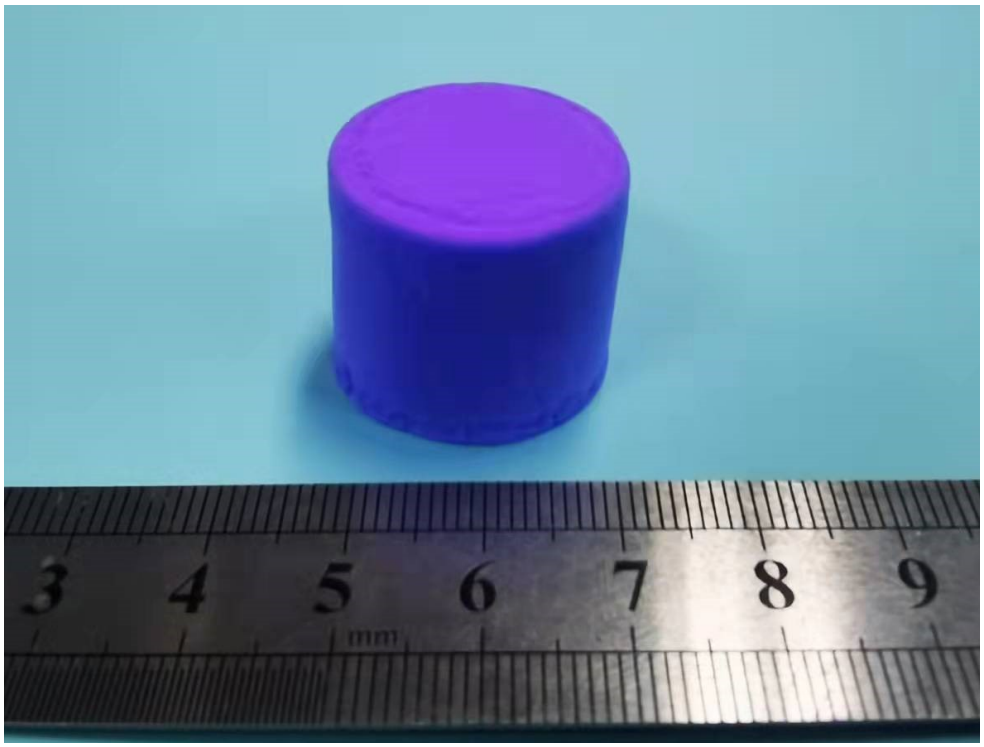

Figure S10 Photograph of the ZIF-67/NFAs.

Table S1 Textural parameters and density of C-ZIF-8-CNFAs and CNFAs

Samples	BET surface area ($m^2\ g^{-1}$)	Pore volume ($cm^3\ g^{-1}$)	Density ($mg\ cm^{-3}$)
C-ZIF-8-CNFAs	288.3	0.22	7.3
CNFAs	12.1	0.01	20.7

Table S2 The percentage of total nitrogen and their types in the C-ZIF-8-CNFAs

Sample	Total N content (%)	Pyridinic-N (%)	Pyrrolic-N (%)	Graphitic-N (%)	Oxidized-N (%)
C-ZIF-8-CNFAs	7.4	2.83	0.96	2.63	0.98

Table S3 Atomic percentage (at%) of C, O and N in C-ZIF-8-CNFAs and CNFAs

Samples	C content (%)	N content (%)	O content (%)
C-ZIF-8-CNFAs	84.8	7.4	7.8
CNFAs	79.8	6.1	14.1